IEEE Open Journal of
Antennas and Propagation

Received 3 August 2023; revised 24 September 2023; accepted 26 September 2023. Date of publication 5 October 2023; date of current version 2 November 2023.

Digital Object Identifier 10.1109/OJAP.2023.3322382

New Analysis and Design Techniques for Arbitrary Reactance Trap Dipoles

PAUL R. WINNIFORD [1,2] (Member, IEEE), ADRIAN L. BAUER [1,2] (Student Member, IEEE), HJALTI H. SIGMARSSON [1,2] (Senior Member, IEEE), AND JESSICA E. RUYLE [1,2] (Senior Member, IEEE)

[1] School of Electrical and Computer Engineering, The University of Oklahoma, Norman, OK 73019, USA

[2] Advanced Radar Research Center, The University of Oklahoma, Norman, OK 73019, USA

CORRESPONDING AUTHOR: J. E. RUYLE (e-mail: ruyle@ou.edu)

This work was supported by the Department of the Navy, Office of Naval Research (ONR) under Award N000141812035.

ABSTRACT The work presents a significantly revised analysis of a classic resonator loaded antenna – the trap dipole. The authors demonstrate in calculation, simulation, and measurement that trap dipoles antennas are not matched or resonant at the same frequency as the trap load resonance. The new analysis unites traditional high impedance trap loads with a wide variety of resonant and reactive loads to achieve multiband antenna performance with quasi-first order field distributions at the operating frequencies. The revised analysis enables the trap dipole to be expanded into a new framework for the design of a wide variety of multi-band or reconfigurable resonator loaded antennas.

INDEX TERMS Dipole antennas, loaded antennas, multifrequency antennas, trap dipoles.

I. INTRODUCTION

THE TRAP-LOADED dipole is a multiband antenna with pairs of bandstop resonator "traps" tuned to higher operating frequencies as shown in Figure 1. The theory of trap dipole antennas underlies a broad class of resonantly loaded antennas [1], [2], [3], [4], [5], [6], [7], [8], [9], [10], [11], [12], [13], [14], [15], [16], [17], [18], [19], [20]. Trap dipoles originated in the amateur radio community [6], [20], so while they are occasionally mentioned in more traditional sources [21], most references are outside of standard antenna literature [22], [23]. It has been traditionally understood that the resonators on a trap dipole create an open-circuit type boundary condition so that the antenna appears shorter and resonates at a higher operating frequency in addition to that corresponding to the full length of the dipole [21]. There have been allusions to the use of the traps as reactive rather than resonant loads in the amateur radio community [24], but always as an alternative to the more common use and understanding of the traps as an open circuit condition. In this paper we show that the trap dipoles never operate when the traps are an open circuit, and only operate when the traps present a reactive load.

There is evidence in the literature that trap dipoles, and resonator loaded antennas by extension, have low radiation efficiency [22], [23]. To date, there has not been a clear explanation of this loss behavior. The majority of trap related publications make no mention of loss or radiation efficiency, even though it is well established in [25] that bandstop resonators introduce maximum dissipation at resonance. From our analysis of trap dipole behavior, presented in this paper, it becomes clear that the low efficiency of trap dipoles stems from a compressed higher-order mode that arises due to heavy reactive loading conditions. Based on this new analysis, we present alternative designs to the classic trap dipole antenna that move the band of low-efficiency performance away from the operating bands of the trap dipole.

In Section II, we present a new analysis of the trap dipole antenna. The model is verified with calculation and simulation in this section, and the results are explained analytically. The new model highlights and explains the occurrence of loss in resonator loaded antennas as being due to loaded higher order modes that are excited by heavy reactive and resonant loading. The contribution of this analysis is to expand trap dipoles from a relatively narrow design into

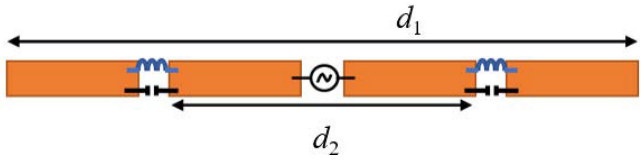

FIGURE 1. Dual-band trap dipole with inductor-capacitor pair "trap" loads. The conventional trap-loaded dipole has an outer length d_1 that is $\lambda/2$ at the lower operating frequency f_1. A pair of bandstop resonator "traps" tuned to a higher operating frequency, f_2, are added to the antenna with $\lambda/2$ spacing at f_2 (marked d_2).

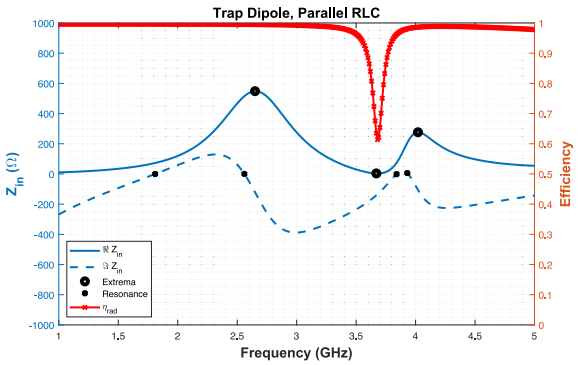

FIGURE 2. Z_{in} and η_{rad} of parallel LC trap dipole antenna, antenna series resonance marked at 1.81 GHz and 3.84 GHz. Both η_{rad} and R_{11} have a minimum at 3.67 GHz, slightly below antenna upper resonance.

a much broader framework for designing novel resonator loaded antennas. This more nuanced understanding of trap dipole behavior opens up new design possibilities for this broad class of antennas, and better accounts for radiation efficiency phenomena and provides strategies for moving spectral nulls in radiation efficiency to more desirable locations. In Section III, we present alternative loading methods that move these lossy modes to frequencies far from the antenna's operating bands. Section IV presents measured results that validate the analysis of Section II and the novel designs of Section III. The conclusion in Section V discusses how the improved method presented in this paper may be generalized to the broad class of resonantly loaded antennas.

II. A NEW ANALYSIS OF TRAP ANTENNAS

We compare the behavior of loaded dipoles with different load locations, values, and types. The impedance parameters and radiation efficiency of trap dipoles are compared to assess loss behavior. In Fig. 2, the input impedance of a typical trap dipole with $d_1 = 75$ mm and $d_2 = 43.8$ mm is overlaid with the radiation efficiency. The antenna resonances in the figure are marked on the reactance curve, and the minima and maxima of the input resistance are also marked in Fig. 2. The dipole is impedance matched near resonance to a 73 Ω source at a lower frequency, f_1 (1.81 GHz), and at an upper frequency f_2 (3.84 GHz), as shown in Fig. 3. The trap is a parallel combination of a 1 nH inductor and a 1.6 pF capacitor and is resonant at f_{trap} (3.98 GHz). There is a significant dip in radiation efficiency below the dipole upper resonance (3.67 GHz), as suggested by [22] and [23].

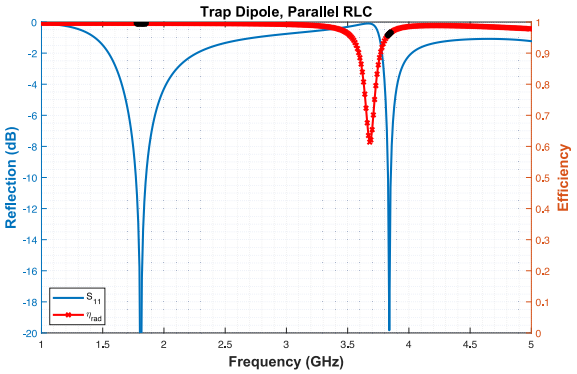

FIGURE 3. S_{11} and η_{rad} of trap dipole antenna, S_{11} is −27 dB at 1.81 GHz and −20 dB at 3.84 GHz. LC trap is resonant at higher frequency 3.98 GHz, and presents a reactive load at f_2.

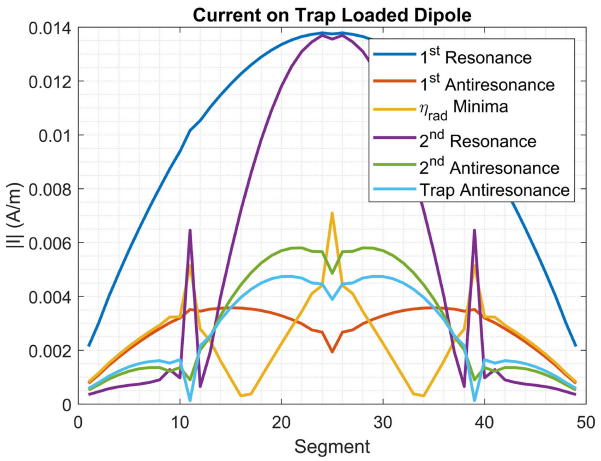

FIGURE 4. Current distribution at key frequencies across trap dipole antenna and calculated with Method of Moments, wire segment numbers displayed, trap loads are at 11 and 39, and the feed is at 25. The operating frequencies are quasi-first mode distributions, and the η_{rad} minimum is a compressed third order mode.

However, the efficiency dip does not align with the antenna upper operating frequency as seen in Fig. 2.

The frequency of minimum radiation efficiency is not the same frequency as the trap resonance, so the resonator is not unavoidably lossy at its resonance, even though it is known that a bandstop resonator introduces loss at resonance [25]. Instead, the radiation efficiency minimum was tied to the minimum value of radiation resistance, and this was consistent for a wide variety of trap dipoles. To illustrate this, the minimum value of the input resistance is marked in Fig. 2 and coincides with the minimum value of the radiation efficiency. The loss resistance, due to copper and dielectric loss as well as load loss is fairly constant over the frequency band, so a low input resistance means that the ratio of the radiation resistance to the loss resistance and therefore radiation efficiency becomes unfavorable. This is not a complete explanation though. To understand the cause of the radiation efficiency dip, which again is not due to lossy trap resonance, we look at the dipole current distribution in Fig. 4. At the radiation efficiency minima, the yellow trace is essentially a 3λ/2 mode, which typically is excited at a much

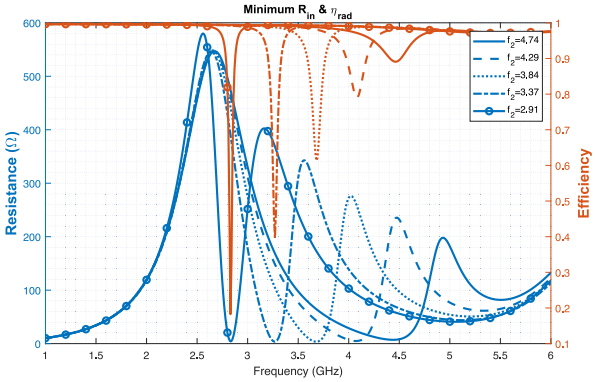

FIGURE 5. Results for trap dipoles with varied f_2 tuning showing η_{rad} minimum dependent on R_{in} minimum. Loss is caused by a compressed higher order $3\lambda/2$ mode that is heavily loaded by the traps. As the dipole is more heavily loaded, the η_{rad} minimum lowers, and all modes are compressed, which results in the antenna antiresonance having a higher Q and therefore a larger peak in real impedance.

TABLE 1. Trap dipole upper operating frequency (f_2) not equal to trap resonant frequency (f_{trap}), dipole outer length constant, load value and load spacing varied.

f_{trap} (GHz)	f_2 (GHz)	d_2 (mm)
5.03	4.74	37.5
4.50	4.29	40.6
3.98	3.84	43.8
3.47	3.37	50.0
2.96	2.91	56.3

higher frequency on an unloaded dipole. The addition of the trap loads significantly lowers the frequency of excitation of the third mode [26], so that it is electrically compressed and has poor radiation efficiency – similar to electrically small antennas. In Fig. 5, several trap dipoles were simulated with different upper operating frequencies, illustrating the radiation efficiency minimum aligning with the input resistance minimum. As the upper operating frequency, f_2, is lowered, the dip in radiation efficiency degrades, which is well explained by the lossy higher order mode being increasingly compressed. All of the resonances are compressed as well, which results in a larger maximum resistance value at the antenna first antiresonance.

More significantly, the antenna second series resonance (3.84 GHz) is not at the same frequency as the trap resonance (3.98 GHz). Surprisingly, this means that the antenna second series resonance is caused by a finite reactive load value, rather than the common assumption that the load is resonant and creating an open circuit boundary condition. This result is consistent over a broad range of trap dipole designs, and the frequency separation between trap resonance and antenna upper resonance is shown in Table 1 for trap dipoles with different upper operating frequencies. The second series resonance frequency was adjusted by changing both the trap resonance and trap spacing. When the load Q is very high, the range of useful load reactance values are very near to the load resonance, so the traditional theory is often close enough for the discrepancy to remain unnoticed in terms of the upper operating frequency. However, extending the principles of trap antenna design to use new load technologies and placements can result in the discrepancy becoming much more significant.

The current distributions at the operating frequencies are also plotted in Fig. 4. The blue trace shows the expected first-order mode at the first resonance, and the purple trace shows a first-order-like current distribution between the trap loads at the second resonance (current spikes at trap load edge). In reality, a combination of higher order modes define the distribution at the antenna second series resonance. The traditional trap dipole understanding approximates the complicated modal interaction to create a useful current distribution without the need for a modal analysis. A current distribution characterized by a low-order mode is a good predictor that the radiation pattern will not have any unwanted beam splitting or other distortions. Importantly, the significant dip in radiation efficiency that consistently appears right below the upper operating band of the classic trap dipole antenna, is due to the excitation of an electrically compressed higher-order mode rather than resonator loss, as has been previously posited [22], [23]. It can be intuitively understood from literature on electrically small antennas and characteristic mode theory [27], [28] that electrically compressed higher order modes will have a poor radiation efficiency.

III. NOVEL TRAP ANTENNAS

The classical trap-loaded dipole is conceptualized as a resonator loaded antenna that has a first-mode-like current distribution at its operating frequencies and does not require complicated modal tracking to achieve the quasi-first mode response at the upper operating frequency. A first mode distribution ensures that the antenna has a desirable radiation pattern despite the full antenna length being electrically large at upper frequencies. With the new analysis that the trap loads are not resonant at the antenna upper resonance, the trap-style antenna can be created with a variety of different reactive loads. All of these details combined makes the trap antenna suitable as a more general template for multiband resonator loaded antennas that are still simple to design.

The term “trap” has typically been used to refer to parallel LC circuits, which present a high impedance to the antenna currents near the circuit resonance. Inductor coils have also sometimes been referred to as traps when they significantly alter the current on feeds and antennas. We choose to use the term “trap” as a general term not just for parallel LC loads, but also for series LC, inductors, and any loads used to present a high impedance at one of the antenna operating frequencies.

The trap dipole upper resonance depends on a reactive open from the trap rather than an actual open, so an inductor load can replicate the upper resonance response. Likewise, since the radiation efficiency minimum is due to a compressed third mode instead of trap resonator loss, the modal behavior at the radiation efficiency minimum frequency can be recreated with just an inductive load, which

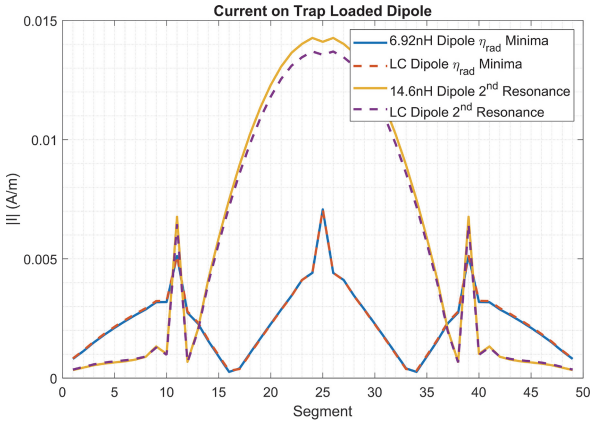

FIGURE 6. The trap dipole current distribution at the second series resonance and at the radiation efficiency minimum in Fig. 4 can be recreated with inductive loads tuned to match the trap reactance at the same frequency. The trap dipole second operating frequency and radiation efficiency minimum are both recreated with excellent agreement, Method of Moments solution with dipole segments labelled.

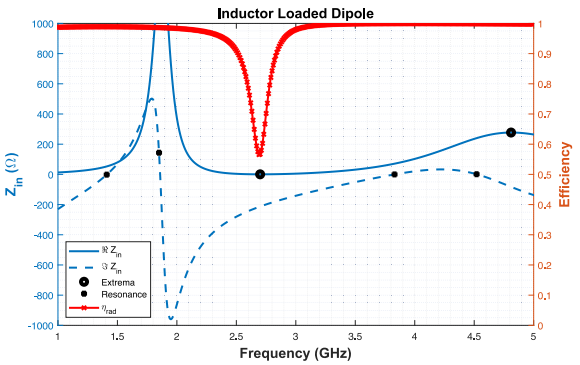

FIGURE 7. Z_{in} and η_{rad} of novel dual-band inductor loaded dipole, based on classic parallel LC trap loaded dipole. Pure inductive load calculated to present the same reactive load as the traditional parallel LC trap at f_2. Dip in η_{rad} at the same frequency as the R_{in} minimum.

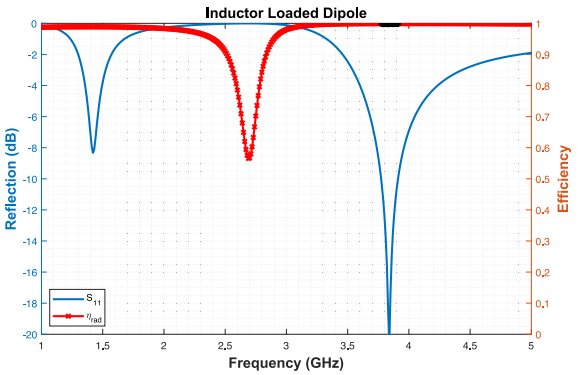

FIGURE 8. S_{11} and η_{rad} of novel dual-band inductor loaded dipole, based on classic parallel LC trap loaded dipole. Dip in η_{rad} does not overlap with upper operating frequency.

is counter to the understanding that trap dipoles have an open circuited load. Both of those scenarios are simulated and shown in Fig. 6. Unlike classic electrically small inductor loaded dipoles and monopoles, the dual band dipoles considered here are near to $\lambda/2$ in length at the lower operating frequency, or 0.36λ to 0.42λ for the cases the authors calculated. The point is that the inductor is not placed near the feed, so it minimally impacts the antenna with a first mode current distribution, but does have a high impact on returning the higher order modes.

At the frequency of the radiation efficiency minima of the example trap loaded dipole, the trap load reactance is j160 Ω. At 3.68 GHz, the reactance corresponds to an inductance of 6.92 nH. In simulation, we loaded a dipole with 6.92 nH inductors to lower the frequency of the resonances. The radiation efficiency minimum occurs with the characteristic third mode distribution, as shown in Fig. 6, and exactly matches that of the parallel LC loaded dipole.

The second operating frequency of the example LC trap dipole is at 3.84 GHz. At 3.84 GHz, the LC resonator has a reactance of j352 Ω, which can be replicated with a 14.6 nH inductor. The first series resonance is tuned lower than in the trap dipole, down to 1.41 GHz, due to the increased inductance shown in Fig. 7. The second series resonance very closely matches that of the trap loaded dipole, with the characteristic quasi-first-mode distribution between the loads, as seen in Fig. 6.

The inductor loaded dual-band dipole proves that the trap loaded dipole experiences a strongly reactive discontinuity from the trap loads at second resonance rather than an actual open circuit condition. The simple inductor loads were calculated to match the parallel LC load values at the upper resonance, and consequentially a new dual-band trap-style antenna was created as seen in Fig. 8.

Since we proved that the upper operating frequency is caused by a reactive load value rather than an actual open circuit boundary condition, we can expand the design process even further as a framework for the design of multiband antenna with arbitrary resonator loads. The parallel LC loads can be replaced with series LC loads. This design is flipped from the original trap design because a series trap LC is a short circuit rather than an open circuit at resonance. To minimally disturb the fundamental resonance of the antenna, the series trap is designed to be resonant near the desired lower operating frequency. The L/C ratio is then selected so that the resonator provides that same j352 Ω at the 3.84 GHz upper operating frequency. A 20 nH and 0.31 pF load is used, which is resonant at 2.02 GHz.

The antenna second series resonance is recreated, and we have a novel dual band resonator loaded antenna, with the dip in radiation efficiency further from resonance as shown in Fig. 9 and 10. The design of trap antennas has been expanded to accommodate parallel or series resonator loads, or simple inductive loads. More complex loads can be incorporated based on simple reactive equivalence with a prototype parallel LC loaded design. It should be noted that the inductor and series trap designs move the radiation efficiency minima much farther away from the operating frequencies of the antenna.

To summarize, a suggested antenna design process using the improved theoretical understanding of trap loaded antenna presented in this paper is as follows. First, a

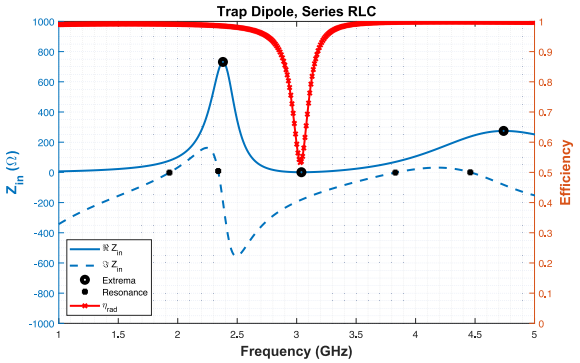

FIGURE 9. Z_{in} and η_{rad} of novel dual-band series LC loaded dipole. Antenna resonances are at 1.93 GHz and 3.83 GHz, and trap resonance at 2.02 GHz. Trap antenna upper frequency f_2 is based on reactive load condition and is not at trap resonance. Series load presents a low impedance at f_1.

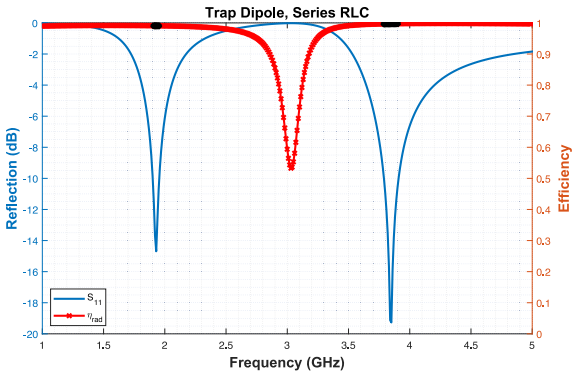

FIGURE 10. S_{11} and η_{rad} of novel dual-band series LC loaded dipole. Series LC load calculated to present the same reactive load value as the traditional parallel LC trap at f_2.

traditional trap dipole is loaded with an antiresonant (parallel resonance) load in the classically understood method for trap dipole design. The outer length is approximately half a wavelength at the lower operating frequency, inner placement of the loads is chosen so that d_2 is less than half a wavelength at the higher operating frequency, and the loads are tuned to resonate at the higher operating frequency. For the trap style antenna newly proposed in this paper, with series LC loads, d_1 should be half a wavelength at the center frequency, with the load resonance tuned to the lower frequency, and the d_2 inner spacing half a wavelength at higher frequency. The exact load placement and L/C ratio tunes the exact value of higher frequency. For the dual resonance trap style antenna with just an inductive load that is newly proposed in this paper, it has an outer length less than half a wavelength at low frequency (we calculated cases as large as 0.42λ), and an inductive load placed around the midpoint of the antenna arms, with exact values impacting f_1 and more strongly impacting f_2. The authors used a custom MoM code in MATLAB, but a loaded dipole also solves quickly in a commercial solver such as HFSS. If desired, the parallel resonator case can be used as a starting point to calculate exact reactance values for the series resonator and inductor loading options. If all three dipoles have the same load placement and same reactance value at f_2, their performance will be identical at f_2.

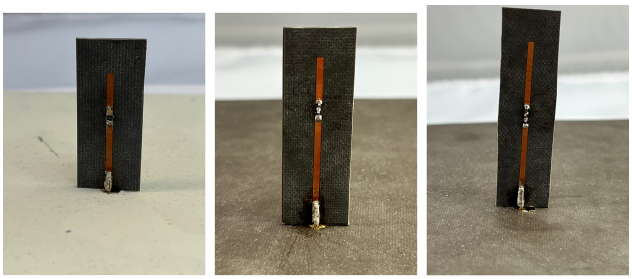

FIGURE 11. Fabricated trap monopoles with (a) parallel LC load, (b) series LC load, and (c) inductive load.

IV. EXPERIMENTAL VERIFICATION

The parallel LC trap antenna, the inductor dual-band trap style antenna, and the series LC trap antenna were all fabricated to further validate our revised analysis and new design procedure. Monopoles were fabricated rather than dipoles for ease of fabrication and measurement as monopoles do not require baluns. The fabricated designs were optimized for available inductors and capacitors and differ in tuning from the previous simulated designs. The fabricated parallel LC trap monopole antenna has a 1 nH inductor and a 1.6 pF capacitor, which are both 0402 surface mount components. The components are soldered to a ribbon radiator on a 31-mil-thick Rogers RT/duroid 5880 substrate and are shown in Fig. 11. The radiators were etched through a photolithography process. The ground plane substrate is a 60 mil Rogers 4350B board and is 6" × 6", which is approximately λ × λ at 2 GHz. The ground plane substrate thickness and material have minimal impact on the antenna, but should be selected to be rigid. The ground plane's length and width have a significant impact on the input resistance magnitude at resonance. The ribbon monopole with a λ × λ ground plane at the lower 2 GHz resonance had a simulated input resistance of 33 Ω, which is near to the ideal value of 36.5 Ω. All of the fabricated monopoles have 0402 sized components on a ribbon radiator, with λ × λ sized ground planes based on the lower operating frequency. The components have self resonant frequency (SRF) above the measured frequencies, and the component tolerance analysis takes into account the component deviation across frequency as provided by the manufacturers.

The parallel LC loaded monopole has operating frequencies at 2.37 GHz and 3.786 GHz, as shown in Fig. 12. At the lower band, the antenna is resonant at 2.11 GHz and antiresonant at 2.55 GHz. The broad impedance match is centered in between the resonance and antiresonance. The upper band is slightly capacitive and does not pass through resonance. The antenna operating frequencies and load values at f_1 and f_2 are listed in Table 2. Trap antennas operate at reactive load conditions and not at

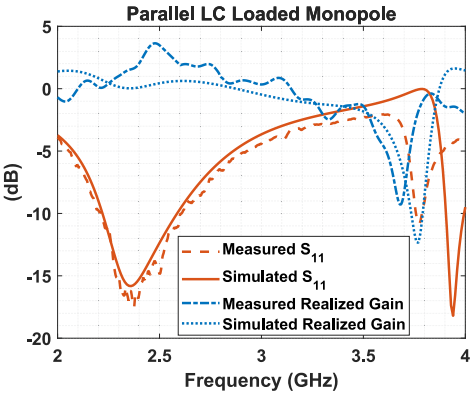

FIGURE 12. Measured parallel LC trap monopole, S_{11} −17.5 dB at 2.37 GHz and −10.8 dB at 3.77 GHz, max realized gain over frequency. Trap antenna f_2 is at reactive load condition and not at trap resonance. Dip in realized gain below f_2 predicted by electrically compressed higher order mode.

TABLE 2. Measured operating frequencies of trap monopoles compared with trap load resonance, including novel series LC and inductor loaded dual-band trap antennas (X_L is the load reactance).

	f_1 (GHz)	X_L $j\Omega$	f_2 (GHz)	X_L $j\Omega$	f_{trap} (GHz)
Parallel LC	2.37	17	3.77	85	4.29
Inductor	1.40	183	3.16	514	X
Series LC	1.43	-45	3.22	693	1.54

trap resonance. The antenna upper operating frequency is 0.51 MHz below the expected trap resonance, though the separation can be as small as 0.38 MHz or as great as 0.65 MHz according to the component tolerance range.

The parallel LC loaded monopole peak realized gain is also shown in Fig. 12. The realized gain, which is impacted by radiation efficiency, has a significant dip below the upper operating frequency, which aligns with the poor radiation efficiency trends seen in simulation. The antenna has typical monopole radiation patterns at both frequencies, as seen in Figs. 13 and 14. While the trends in peak realized gain shown in Figure 12 agree between simulated and measured results, there is some ripple in the measured results due to typical measurement error such as multipath propagation in the anechoic chamber and frequency shifts due to manufacturing and component tolerances.

The inductor loaded monopole and the series LC loaded monopole antennas were both designed at slightly lower frequencies in order to accommodate the SRF limits of the inductors and capacitors. The fabricated inductor loaded monopole has a 20 nH inductor load. The dual-band inductor loaded monopole has a lower operating frequency at 1.4 GHz and an upper operating frequency at 3.16 GHz, seen in Fig. 15. The antenna is resonant at 1.36 GHz, near to the first operating frequency, and is antiresonant at 3.19 GHz, which is near to the second operating frequency. The antenna also has a dip in realized gain corresponding to the expected dip in radiation efficiency. This additionally confirms that even though trap antennas have lossy frequencies, the loss is not due to resonator loss.

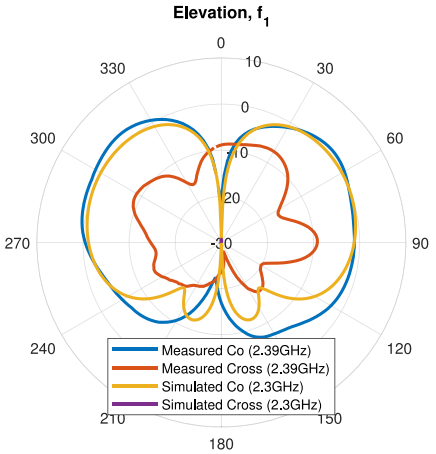

FIGURE 13. Parallel LC trap monopole, measured 1.3 dB realized gain at f_1, −7 dB cross-polarization. Agrees with simulation data. Typical monopole radiation patterns resulting from quasi-first-order modes at both f_1 and f_2.

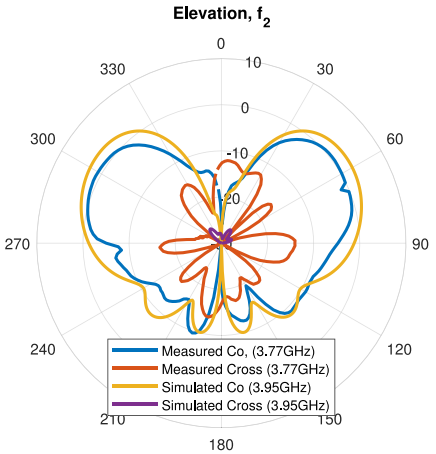

FIGURE 14. Parallel LC trap monopole, measured 0.8 dB realized gain at f_2, −12 dB cross-polarization. Agrees with simulation data. Typical monopole radiation patterns resulting from quasi-first-order modes at both f_1 and f_2.

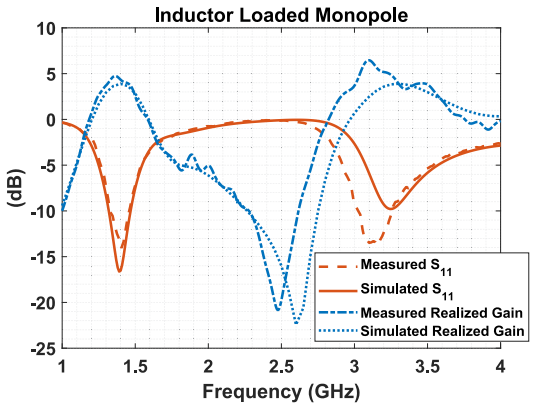

FIGURE 15. Measured novel dual-band inductor "trap" monopole, S_{11} and max realized gain over frequency. Dual-band trap dipole behavior can be created with an appropriately large inductor load.

The inductor loaded monopole has clean monopole radiation patterns at both operating frequencies seen in Fig. 16 and 17. The measured inductor loaded monopole

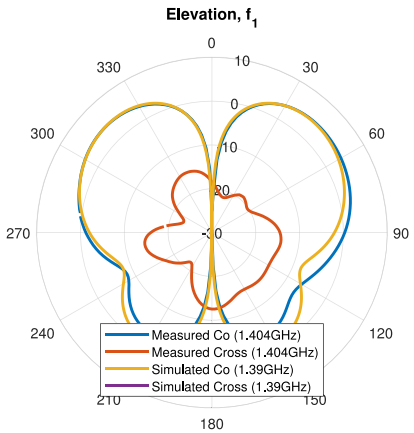

FIGURE 16. Dual-band inductor "trap" monopole, measured and simulated E-plane co-polarized realized gain at f_1.

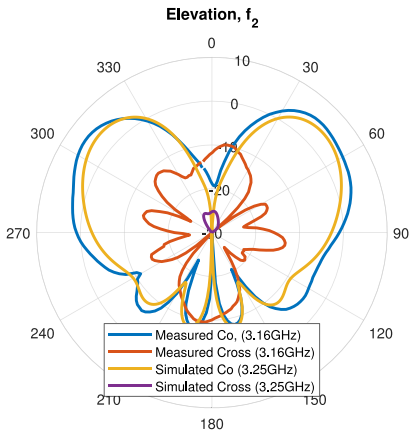

FIGURE 17. Dual-band inductor "trap" monopole, measured and simulated E-plane co-polarized realized gain at f_2.

demonstrates that a simple inductor load can be used to achieve trap antenna dual-band performance. This verifies the revised understanding of trap antennas being based on reactive loads and verifies that the loss-band on the loaded antenna is not the consequence of increased loss at load resonance, but is better explained as the occurrence of heavily loaded and electrically compressed higher order modes.

The fabricated series LC loaded monopole has a 0.3 pF and 30 nH trap. The series trap monopole has operating frequencies at 1.43 GHz and 3.22 GHz, as seen in Fig. 18. The load is resonant at 1.68 GHz, so it adds a small capacitance to the monopole at the lower 1.43 GHz operating frequency, and adds a larger inductance at the 3.22 GHz operating frequency. The lower operating frequency is nearly resonant, with the first antenna resonance at 1.4 GHz. The upper operating frequency is in between an antenna resonance at 2.86 GHz, and an antiresonance at 3.34 GHz.

The dip in realized gain is seen also in the series trap in Fig. 18, demonstrating the prevalence of lossy frequencies regardless of load type. The antenna also still has typical monopole radiation patterns, so the dual first-mode like behavior of trap dipoles can be replicated with a variety

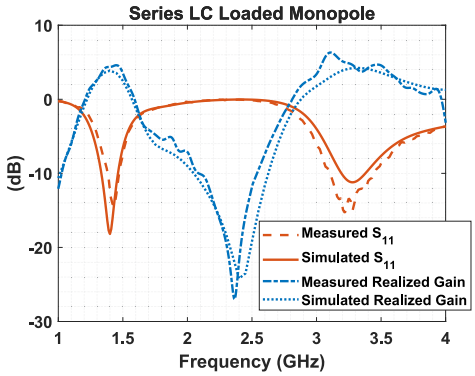

FIGURE 18. Measured novel series LC trap monopole, S_{11} and max realized gain over frequency.

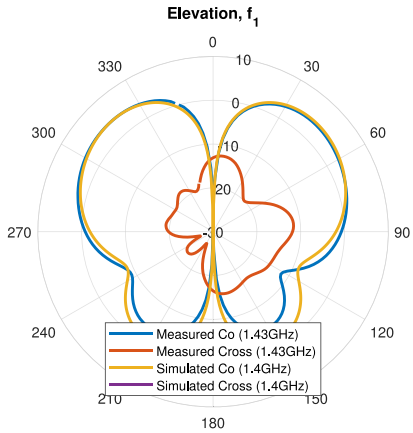

FIGURE 19. Series LC trap monopole, measured and simulated E-plane co-polarized realized gain at f_1.

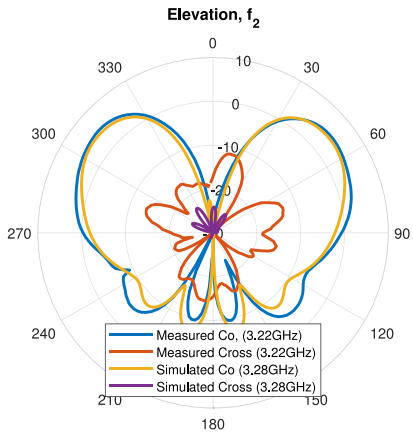

FIGURE 20. Series LC trap monopole, measured and simulated E-plane co-polarized realized gain at f_2.

of load types. The series LC loaded monopole has typical monopole radiation patterns at both operating frequencies, shown in Figs. 19 and 20.

The novel series LC trap antenna and the dual band inductor loaded trap-style antenna have been fabricated and operate as expected. These new designs are based on the revised understanding that trap loads are reactive and not

resonant at the trap antenna upper resonance. In all three of the fabricated dual-band trap antennas, the load is not resonant at the antenna operating frequency. The designs are proof of the revised theory. The realized gain measurements also show the existence of a loss band that has been explained as the excitation of an electrically compressed higher order mode. If the antenna is designed correctly, the loss is not at the antenna operating frequencies.

V. CONCLUSION

A revised and more accurate analysis of the longstanding trap dipole antenna has been presented and experimentally verified. Contrary to previous understanding, the trap loads are not resonant at the antenna upper band resonance, but instead provide reactive loading. This significantly relaxes the conditions for designing the multiband trap antenna, and any matching reactive load can be substituted. We leveraged this finding to expand the simple design process for trap dipoles into a design framework for trap antennas as a broad new class of high-efficiency resonator loaded multiband antennas. The existence of loss - which has been occasionally mentioned in the literature - has been demonstrated and the loss has been explained as being due to the excitation of an electrically compressed higher order mode. Techniques for designing efficient trap loaded antennas are shown - including a series and inductively loaded trap dipole that push the efficiency null far from the operating frequencies of the antenna, unlike the classic parallel trap dipole antenna. Furthermore, being able to tune the location of a radiation efficiency null through load choice means that the null can be used beneficially as a spectral mask.

Novel multiband antennas can be designed to have quasi-first-mode current distributions at multiple frequencies, with reactive or resonant loads, based on a simple trap dipole prototype design. Antennas with more complex and reconfigurable loads such as MEMS and varactor based resonators can be designed by optimizing the load reactance to match the LC prototype designs in this paper. The design process is a simple framework that removes the need to explicitly analyze the complex modal behavior resulting from the load structures, and still delivers excellent radiation efficiency.

REFERENCES

[1] M. Bulgerin and A. Walters, "Small antenna investigation," NOLC, Washington, DC, USA, Rep. 154, 1954.

[2] A. Fourie and B. Austin, "Improved HF broadband wire antenna," *Electron. Lett.*, vol. 23, no. 6, pp. 276–278, 1987.

[3] J. Hall, "Off-center-loaded dipole antennas," *QST*, vol. 58, pp. 28–34, Sep. 1974.

[4] C. E. Smith, "A critical study of two broadcast antennas," *Proc. Inst. Radio Eng.*, vol. 24, no. 10, pp. 1329–1341, 1936.

[5] H. A. Wheeler, "Fundamental limitations of small antennas," *Proc. IRE*, vol. 35, no. 12, pp. 1479–1484, Dec. 1947.

[6] C. Buchanan, "The multimatch antenna system," *QST*, vol. 130, pp. 22–23, Mar. 1955.

[7] D. D. Reuster and K. J. Cybert, "A high-efficiency broadband HF wire-antenna system," *IEEE Antennas Propag. Mag.*, vol. 42, no. 4, pp. 53–69, Aug. 2000.

[8] A. Mirkamali, P. S. Hall, and M. Soleimani, "Reconfigurable printed-dipole antenna with harmonic trap for wideband applications," *Microw. Opt. Technol. Lett.*, vol. 48, no. 5, pp. 927–929, 2006.

[9] A. Mirkamali, P. S. Hall, and M. Soleimani, "Wideband reconfigurable printed dipole antenna with harmonic trap," in *Proc. IEEE Int. Workshop Antenna Technol. Small Antennas Novel Metamater.*, 2006, pp. 188–191.

[10] W. O. Coburn and C. Fazi, "A lumped-circuit model for a triband trapped dipole array-part II: Stacked arrays," *IEEE Antennas Wireless Propag. Lett.*, vol. 7, pp. 648–651, 2008.

[11] W. O. Coburn and C. Fazi, "A lumped-circuit model for a triband trapped dipole array-part 1: Model description," *IEEE Antennas Wireless Propag. Lett.*, vol. 8, pp. 14–18, 2009.

[12] R. Anwar, N. Misran, M. T. Islam, and G. Gopir, "Compact multiband VHF antenna for transient radio telescope," in *Proc. Int. Conf. Space Sci. Commun.*, 2009, pp. 182–185.

[13] P. Taylor, J. C. Batchelor, and E. A. Parker, "Dual-band FSS design using LC traps," in *Proc. Loughborough Antennas Propag. Conf.*, 2010, pp. 405–408.

[14] H. Ayad, A. Khalil, M. Fadlallah, F. Ndagijimana, and J. Jomaah, "Design of MSRR-loaded dual-band dipole PCB antennas," in *Proc. ICT*, 2013, pp. 1–5.

[15] F. Parrini, F. Papi, and M. Pieraccini, "Double resonance L-C trap for dual-band dipole antenna," in *Proc. IEEE Conf. Antenna Meas. Appl. (CAMA)*, 2014, pp. 1–4.

[16] M. A. Antoniades and G. V. Eleftheriades, "Multiband compact printed dipole antennas using NRI-TL metamaterial loading," *IEEE Trans. Antennas Propag.*, vol. 60, no. 12, pp. 5613–5626, Dec. 2012.

[17] S. Jamilan, M. A. Antoniades, J. Nourinia, and M. Azarmanesh, "A compact multiband printed dipole antenna loaded with two unequal parallel NRI-TL metamaterial unit cells," *IEEE Trans. Antennas Propag.*, vol. 63, no. 9, pp. 4244–4250, Sep. 2015.

[18] M. M. Zargar, A. Rajput, K. Saurav, and S. K. Koul, "Low radar cross section dipole antenna integrated with absorptive frequency selective reflection structure," in *Proc. 16th Eur. Conf. Antennas Propagat. (EuCAP)*, 2022, pp. 1–4.

[19] K. Saurav, D. Sarkar, and K. V. Srivastava, "CRLH unit-cell loaded multiband printed dipole antenna," *IEEE Antennas Wireless Propag. Lett.*, vol. 13, pp. 852–855, 2014.

[20] H. Morgan, "Multifrequency tuned antenna system," *Electronics*, vol. 13, pp. 42–50, Aug. 1940.

[21] D. Smith, "The trap-loaded cylindrical antenna," *IEEE Trans. Antennas Propag.*, vol. 23, no. 1, pp. 20–27, Jan. 1975.

[22] J. Pemberton, "Multimatch antenna for 'phone," *QST*, vol. 39, pp. 24–25, Dec. 1955.

[23] Y. Beers, "Designing trap antennas: A new approach," *Ham Radio Mag.*, pp. 60–69, Aug. 1987.

[24] *The ARRL Antenna Book for Radio Communications*, 24th ed., Amer. Radio Relay League, Newington, CT, USA, 2019.

[25] G. Matthaei, *Microwave Filters, Impedance-Matching Networks, and Coupling Structures*. Norwood, MA, USA: Artech House, 1980, pp. 775–809.

[26] Y. Luo and Z. N. Chen, "Compressed dipoles resonating at higher order modes with enhanced directivity," *IEEE Trans. Antennas Propag.*, vol. 65, no. 11, pp. 5697–5701, Nov. 2017.

[27] L. J. Chu, "Physical limitations of omni-directional antennas," *J. Appl. Phys.*, vol. 19, no. 12, pp. 1163–1175, 1948.

[28] J. J. Adams, S. Genovesi, B. Yang, and E. Antonino-Daviu, "Antenna element design using characteristic mode analysis: Insights and research directions," *IEEE Antennas Propag. Mag.*, vol. 64, no. 2, pp. 32–40, Apr. 2022.

PAUL R. WINNIFORD (Member, IEEE) received the B.S. degree in electrical engineering and the M.S. and Ph.D. degrees in electrical and computer engineering from The University of Oklahoma in 2013, 2015, and 2020, respectively.

From 2014 to 2020, he was a Graduate Research Assistant with The University of Oklahoma, where he was a member of Advanced Radar Research Center. He has been a Senior Electrical Engineer with Raytheon Technologies since 2021 and designs wideband arrays and passive microwave circuits. His graduate research interests included multifrequency and frequency reconfigurable antennas, and filtering antennas or filtennas for phased array applications.

ADRIAN L. BAUER (Student Member, IEEE) received the B.S. degree in electrical engineering and the M.S. degree in electrical and computer engineering from The University of Oklahoma in 2020 and 2022, respectively.

He is currently a Graduate Research Assistant with The University of Oklahoma, where he is a member of Advanced Radar Research Center. His research interests include frequency reconfigurable antennas and filtering antennas or filtennas.

HJALTI H. SIGMARSSON (Senior Member, IEEE) received the Bachelor of Science degree in electrical and computer engineering degree from the University of Iceland, Reykjavik, Iceland, in 2003, and the Master of Science and Ph.D. degrees in electrical and computer engineering from Purdue University, West Lafayette, in 2005 and 2010, respectively.

He is currently with the School of Electrical and Computer Engineering and the Advanced Radar Research Center, The University of Oklahoma (OU), Norman, OK, USA, where he is an Associate Professor. His current research is focused on reconfigurable RF and microwave hardware for agile communications, measurement, and radar systems. Furthermore, his research interests include spectral management schemes for cognitive radio architectures, advanced packaging utilizing heterogeneous integration techniques, and additive manufacturing of electromagnetic components.

Dr. Sigmarsson was the recipient of the Best Paper Award of the IMAPS 2008 41st International Symposium on Microelectronics. In 2015, he was awarded the Air Force Office of Scientific Research Young Investigator Program to support his research on reconfigurable high-frequency components using phase-change materials. He was named the recipient of the Gerald Tuma Presidential Professorship in 2018 for meeting the highest standards of excellence in scholarship and teaching. For his outstanding support of graduate education, he was awarded the 2021 OU Graduate College Graddy Award. He is an Associate Editor of the IEEE TRANSACTIONS OF MICROWAVE THEORY AND TECHNIQUES and the Editor-in-Chief of the IEEE Microwave Theory and Technology Society (MTT-S) Electronic Newsletter. From 2018 to 2022 he was an Associate Editor of the IEEE MICROWAVE AND WIRELESS COMPONENT LETTERS. In 2019, he was the General Chair for the IEEE Wireless and Microwave Technology Conference (WAMICON) and serves on the WAMICON Executive Committee. In the last decade, he has been involved in multiple conference technical program committees, such as the International Microwave Symposium, the European Microwave Conference, the IEEE Radio Wireless Week, and WAMICON. He is a member of the MTT-S Technical Committee on filters (TC-5).

JESSICA E. RUYLE (Senior Member, IEEE) was born in Shawnee, OK, USA, in 1984. She received the B.S. degree in electrical engineering from Texas A&M University, College Station, in 2006, and the M.S and Ph.D. degrees in electrical engineering from the University of Illinois at Urbana–Champaign in 2008 and 2011, respectively.

From 2006 to 2011, she was a Graduate Research Assistant with the University of Illinois at Urbana–Champaign. From 2012 to 2019, she was an Assistant Professor with the School of Electrical and Computer Engineering, The University of Oklahoma (OU), Norman. In 2019, she was promoted to an Associate Professor of Electrical and Computer Engineering with OU, where she is a member of Advanced Radar Research Center. She holds two patents for her antenna designs. Her research interests are in the development and characterization of new electromagnetic devices and platforms, such as antennas and packaging to improve the performance of radiating systems in challenging environments.

Prof. Ruyle is the recipient of a DARPA Young Faculty Award for her work in highly conformal, placement insensitive antennas and was named a William H. Barkow Presidential Professor at OU. She is an Associate Editor of IEEE ANTENNAS AND WIRELESS PROPAGATION LETTERS. She is a member of Tau Beta Pi and Eta Kappa Nu.